

ADVANCEMENT AND PROMISING DEPICTIONS OF NON LINEAR OPTICAL ORGANIC CRYSTAL 4-NITROPHENOL 8-HYDROXYQUINOLINE (4n8Q) FOR OPTO ELECTRONIC APPLICATIONS

J. VIDHYA *, K.VIJAYAKUMAR, C. PARI

Department of Science and Humanities, M.Kumarasamy College of Engineering, Karur- 639 113, Tamilnadu, India

Single crystals of 4-nitrophenol 8-hydroxyquinoline has grown by slow evaporation solution growth technique at room temperature. The crystal structure and crystallinity of the compound was confirmed by using X-Ray diffraction analysis. Vibrational modes of the functional groups were identified by using FTIR technique. Percentage of C, H and N present in the compound was confirmed by elemental analysis. Optical transmittance spectrum and Band gap was recorded by using UV-Vis-NIR spectrum. Thermal stability of the crystal was evaluated by Thermo Gravimetric and Differential Scanning Calorimetric studies. Dielectric, DC and photoconductivity measurements were also carried out for the grown crystal. The second harmonic generation efficiency of the grown crystal was found to be 7.81 times greater than that of standard KDP. Photoluminescence study was also taken for the grown crystal.

(Received May 22, 2019; Accepted October 10, 2019)

Keywords: Optical materials, Crystal growth, Thermal study, SHG. Electrical conductivity

1. Introduction

In the field of nonlinear optics in the area of material science associated with the optoelectronics device technologies. Organic materials became alternative to inorganic materials. Particularly, materials with aromatic rings have been focused much attention because of their large hyperpolarizability (β), high electronic susceptibility ($\chi^{(2)}$), low cost, fast response time, ease of synthesis and device fabrication [1-6]. In order to get high molecular polarizability, material requires increase in number of π electrons and π delocalization length. 4-nitrophenol is a dipolar NLO chromophore consists of highly delocalized conjugated systems linking donor and the acceptor shows large NLO response. Presence of phenolic OH favours the formation of salts with various inorganic and organic bases. Previously 4-nitrophenol based organic NLO crystals such as Tri-nitrophenol methyl p-hydroxybenzoate, L-Histidinium-4-nitrophenolate 4-nitrophenol, Dimethyl amino pyridinium 4-nitrophenolate-4-nitrophenol, 2,6-diaminopyridinium 4-nitrophenolate-4-nitrophenol, 2-Aminopyridinium 4-nitrophenolate-4-nitrophenol, L-arginine 4-nitrophenolate-4-nitrophenol dehydrate and L-phenylalanine 4-nitrophenol were grown by slow evaporation solution growth techniques [7-16]. 8-hydroxyquinoline is an organic nonlinear optical material in which OH acts as an electron donor and N group acts as an acceptor. Its NLO efficiency is compared with KDP which is 4.78 times higher. Previously its physiochemical and theoretical properties were studied by several workers and also 8-HQ mixed with some organic acids (8-hydroxyquinolinium picrate and 8-hydroxyquinolinium hydrogen maleate) and their NLO properties were already reported [17-22]. On the basis of these facts, in the present communication, for the first time 4-nitrophenol mixed with 8-hydroxyquinoline and the new adduct crystal is grown. 4n8Q is synthesized using 4-nitrophenol and 8-hydroxyquinoline in the ratio of 1:1 and the crystals were grown by slow evaporation solution growth technique. The grown crystals were subjected to elemental analysis, single crystal XRD, powder XRD, UV, FTIR, TG/DSC, dielectric, photoconductivity and powder SHG studies and the results were discussed.

* Corresponding author: opilal@gmail.com

2. Experimental

Material synthesis and crystal growth

Commercially available 4-nitrophenol (Merck 99%) and 8-hydroxyquinoline (Himedia 99%) both reactants were taken in equimolar ratio and dissolved separately using acetone and stirred well for about 20 min. Then the solutions were mixed together and stirred for about 1 hr using magnetic stirrer. The saturated solution was filtered twice using whatman filter paper (No.42 grade) and transferred to 250 ml beaker. To control the solvent evaporation rate, top of the beaker was covered with thin plastic sheet and kept at undisturbed place for slow evaporation. After 4 days good quality crystals were acquired from the mother solution. Quality of the crystals was depicted in Fig. 1.

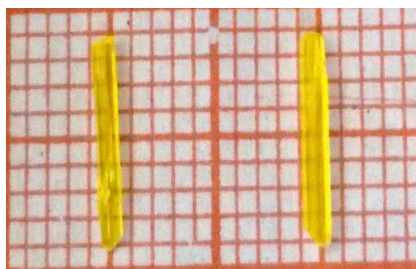


Fig. 1. As grown crystals of 4n8Q.

3. Results and discussion

Elemental analysis

The elemental composition percentage of 4n8Q crystals were determined using Vario EL III Elemental analyser (Germany). The analysed results were given in Table 1. Experimental and theoretical carbon, hydrogen and nitrogen percentages well matches with each other which confirms the presence of compound.

Table 1. Elemental composition percentage of 4n8Q.

| Elements | Experimental (%) | Theoretical (%) |
|----------|------------------|-----------------|
| Carbon | 63.26 | 63.37 |
| Hydrogen | 4.16 | 4.25 |
| Nitrogen | 9.71 | 9.85 |

Single crystal XRD

The as grown single crystals of 4n8Q were subjected to single crystal XRD with MoK α radiation, graphite monochromator; $\lambda=0.71073\text{\AA}$. Results indicate that the titled compound belongs to the triclinic system with a space group of *P1*. The lattice parameter values are found to be $a = 7.6957\text{\AA}$, $b = 12.6780\text{\AA}$, $c = 14.5545\text{\AA}$ and $\alpha=88.99^\circ$, $\beta=82.006^\circ$, $\gamma=81.208^\circ$. The volume of the 4n8Q crystal was found to be $1389.69(\text{\AA}^3)$. Pure 4-nitrophenol and 8-hydroxyquinoline crystals lattice parameters were compared with the 4n8Q and depicted in Table 2.

Table 2. The comparison of cell parameters of pure 4-nitrophenol, 8-hydroxyquinoline and 4n8Q single crystal.

| Lattice parameters | 4-nitrophenol [Ref 23] | 8-hydroxyquinoline [Ref 24] | Present work |
|--------------------|------------------------|-----------------------------|--------------|
| a (Å) | 6.16 | 29.18 | 7.6957 |
| b (Å) | 8.83 | 25.36 | 12.6780 |
| c (Å) | 11.54 | 3.91 | 14.5545 |
| Space group | <i>P21/c</i> | <i>Fdd2</i> | <i>P1</i> |
| System | Monoclinic | Orthohombic | Triclinic |

Powder XRD analysis

Powder X-ray diffraction pattern for the grown crystals were carried out by using Rich seifert diffractometer. Diffraction pattern data were collected on the diffractometer equipped with monochromated CuK α radiation (1.540598Å) and detected by a scintillation counter. The sample was scanned over the 2 theta range of 5-80 $^{\circ}$ at a scan rate of 3/min. Fig. 2 depicts the powder X-ray pattern for the 4n8Q crystal. The characteristic Bragg's peaks at specific 2theta angle testimonies the crystalline nature of the sample. The peak corresponding to (1 2 2) plane has the maximum intensity of 51531 counts per second. The various planes of reflections (hkl) were indexed using TREOR 90 programme.

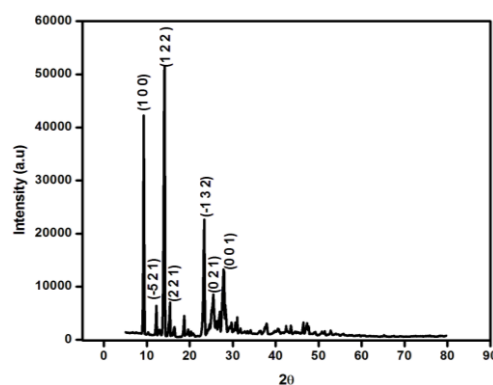


Fig. 2 XRD spectrum of 4n8Q crystal

Optical studies

The optical transmittance spectrum for the grown crystal was recorded using a Perkin-Elmer Lambda 35 Spectrophotometer in the wavelength range from 200-1200 nm. The recorded spectrum is shown in Fig. 3a. The grown crystal has a wider transparency range in the visible and NIR region. From the figure it is observed that the crystal has UV cut-off wavelength at 473 nm and it is assigned to π - π^* transition of the aromatic moiety in the crystal. High transmittance of grown crystal in the visible region facilitates it to be a potential crystal for optoelectronics applications. Grown crystal exhibits good transparency from 470 nm to 1100 nm with the transmittance more than 90 %. The higher optical transmission in solution grown 4n8Q crystal may be due to lesser defects and absence of inclusions, which in turn reduced scattering in 4n8Q crystals and increases the output intensity [25-28]. The optical absorption coefficient (α) was calculated from the transmittance using the given formula

$$\alpha = \frac{2.3036 \log (1/T)}{d} \quad (1)$$

where T is the measured crystal transmittance and d is the thickness of the sample. Assuming parabolic trends, the relation between α and E_g is given by

$$\alpha = \frac{A(h\nu - E_g)^n}{h\nu} \quad (2)$$

where A is a constant, E_g is the optical band gap of the material, ν is the frequency of the incident photon and h is the planck's constant. Fig 3b shows the plot of $h\nu$ and $(\alpha h\nu)^2$. Optical band gap of the material was obtained by extrapolating the linear portion of the plots of $(\alpha h\nu)^2$ and $h\nu$. The optical band gap was found to be 2.97eV. Crystals with wide band gap expected to possess high laser damage threshold and large transmittance in the visible region [7, 29, 30].

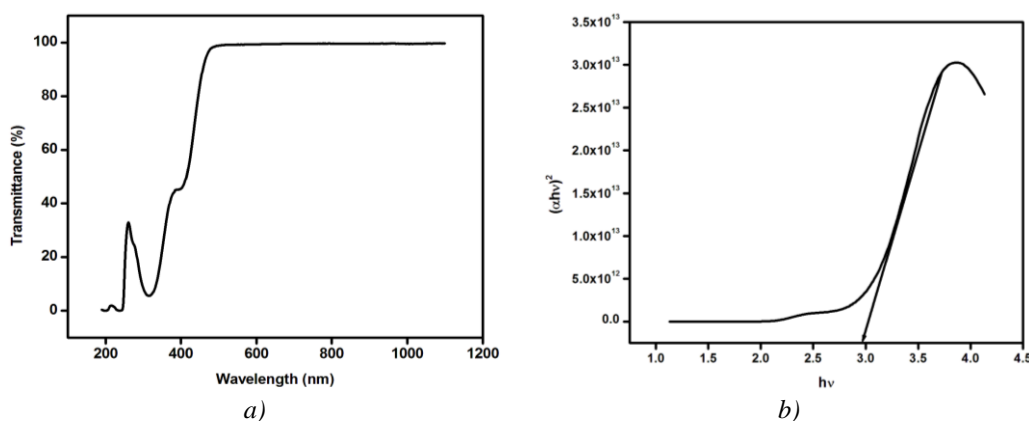


Fig. 3. a) Optical transmittance spectrum of 4n8Q crystal.
b Plot of $h\nu$ Vs $(\alpha h\nu)^2$ 4n8Q crystal.

FTIR studies

The middle infra-red spectrum of the grown crystal was recorded in the wavelength range of 400–4000 cm^{-1} . The recorded spectrum is depicted in Fig. 4. The peaks at 3309, 3055, 2924, 2854 and 2623 cm^{-1} is due to symmetric and asymmetric stretching modes of OH and CH groups. Bands observed at 1280, 1165, 1095, 1064 and 971 cm^{-1} are assigned to in-plane CH bending vibration. Peaks appear at 1496 and 1573 is due to C=C Vibration. Band at 1381, 1496 and 1573 cm^{-1} are due to the symmetric and asymmetric stretching of NO_2 vibration. CN stretching vibration is positions at 810 cm^{-1} . The aromatic C-H stretch vibration is occurred at 3055 cm^{-1} . Vibration at 1494 cm^{-1} is assigned to aromatic ring skeleton vibration. Vibrations at 702, 740, 779, 810 and 848 cm^{-1} are due to CH out of plane bending vibration. The peaks at 702, 632, 578 cm^{-1} are due to OH out-of plane bending vibrations.

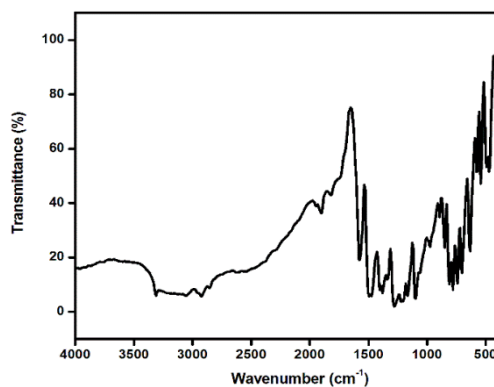


Fig. 4. FT-IR spectrum of 4n8Q crystal.

Dielectric studies

Dielectric measurement is important to study the lattice dynamics of the crystal. Also it provides useful information such as nature of atoms, defects, ions and their bonding as well as polarization mechanism in the materials. Generally dielectric properties are correlated with electro-optic property of the crystal. Measurements were carried out in the temperature ranging from 303K to 335K. Capacitance of the crystal was measured by varying the frequency range 50Hz to 5MHz. The dielectric constant of the crystal was calculated using the obtained capacitance values by the given formula

$$\epsilon_r = \frac{Cd}{\epsilon_0 A} \quad (3)$$

where C is the measured capacitance, d is the thickness of the crystal, A is the cross sectional area of the crystal and ϵ_0 is the free space permittivity of the crystal. Fig. 5a shows dielectric constant Vs frequency for the grown crystal. From the figure it is concluded that dielectric constant is high at low frequency and also it increases with increase in temperature. As the frequency increases dielectric constant value decreases and attains a constant value at very high frequency. Dielectric studies provide useful information concerning dielectric constant thus arises from different polarizations namely electronic, ionic, space charge and orientation. In these polarizations space charge polarization will reckon on the crystalline perfection and quality of the sample. So in the present system it is active at low frequency region and high temperature [31-33]. Fig. 5b shows frequency dependent dielectric loss for the grown crystal. The dielectric loss is very low at high frequency. This low value indicates crystals own good quality with lesser defects which makes it a suitable candidate for optoelectronic applications [34, 35]. In accordance with Miller rule, the lower value of dielectric constant for the grow crystal with higher frequency is a suitable parameter for the improvement of SHG coefficient [36] and electro-optical and microelectronics applications [37, 38].

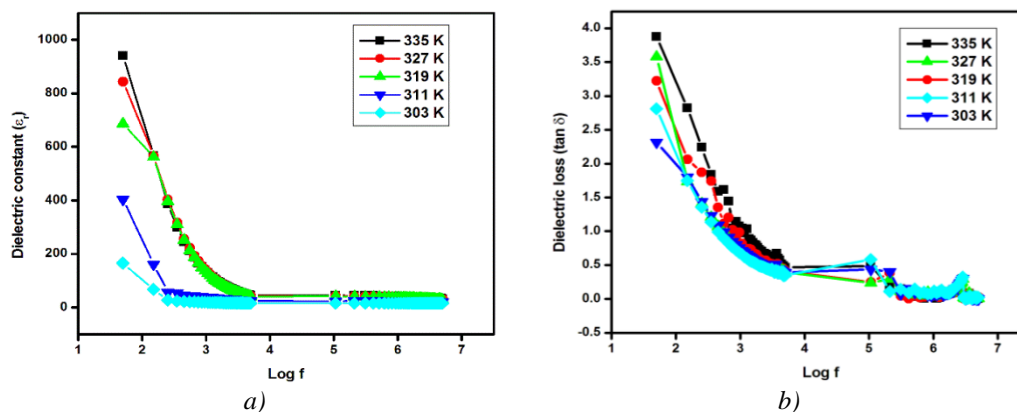


Fig. 5. a) Dielectric constant Vs frequency of 4n8Q crystal.
b) Dielectric loss Vs frequency of 4n8Q crystal.

Photoconductivity

Dark and photocurrent measurements on the harvested crystal were carried out by two probe technique at room temperature. Fig. 6 depicts the dark current and photocurrent response for 4n8Q crystal. From the figure it is visible V-I characteristics of the as prepared sample shown linear with the applied voltage. The photocurrent is higher than dark current which is termed as positive photoconductivity. It may be due to the increase of charge carriers in the presence of illumination of the sample with halogen lamp. Materials with positive photoconductivity nature can be used towards solution wave communications [39].

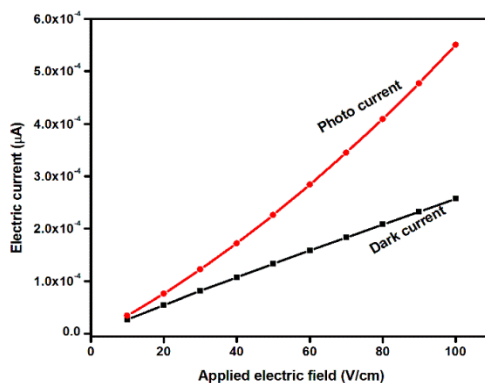


Fig. 6. Photoconductivity response of 4n8Q crystal.

TG/DTA studies

Thermo gravimetric (TG) and differential thermal analysis (DTA) gives useful information regarding phase transition and different stages of decomposition of the compound. To study the thermal stability of the grown crystal TG/DTA analysis were carried out using SDT Q 600V 8.3 instrument from room temperature to 800 °C in nitrogen atmosphere at a heating rate of 20 °C/min. Fig. 7a and 7b shows the TG/DTA analysis spectrum of 4n8Q and pure 4-nitrophenol crystals.

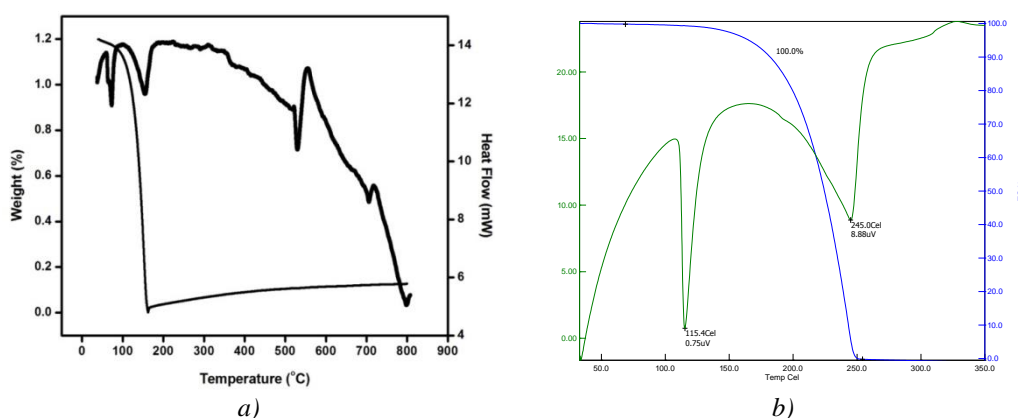


Fig. 7.a) TG/DTA spectrum of 4n8Q crystal.
b) TG/DTA spectrum of pure 4-nitrophenol crystal.

From the TG curve it is observed that the crystal undergoes single stage decomposition occurred between 70 °C to 157 °C which is due to the liberation of volatile substance like NO₂. Also TG curve shows full degradation at 158 °C. In DTA there is a sharp endothermic at 72 °C is assigned to melting point of the compound which are fit well with the TG spectrum. TG curve indicate that there are no endothermic or exothermic transitions below the melting point. This shows that the material is moisture free and stable up to 72 °C. With the temperature increasing above 158 °C volatile substances such as CO, CO₂, CH₄ and NH₃ molecules will be liberated [16]. Fig. 7b shows the TG/DTA spectrum of pure 4-nitrophenol. TG spectrum indicates the single stage decomposition. In DTA sharp endothermic peak at 115 °C assigned to melting point of the compound. Whereas the pure 8-hydroxyquinoline is thermally stable up to 78 °C [40]. A variation in the TG, DTA and melting point confirms the presence of new compound.

Fluorescence studies

The photoluminescence spectrum of the grown crystals was carried out using Varian Cary Eclipse Fluorescence Spectrophotometer in room temperature. The excitation spectrum of 4n8Q crystal was recorded in the range of 200-1100 nm, which is shown in Fig. 8a. Two bands were observed at 237 and 315 nm. Fig. 8b reveals the emission spectrum. The emission peak at 420 and 442 nm attributed to blue fluorescence emission. It is observed that emission intensity suddenly decreases after 442 nm. Strong PL emission indicates that the grown crystal can be useful candidate for optoelectronic applications [41].

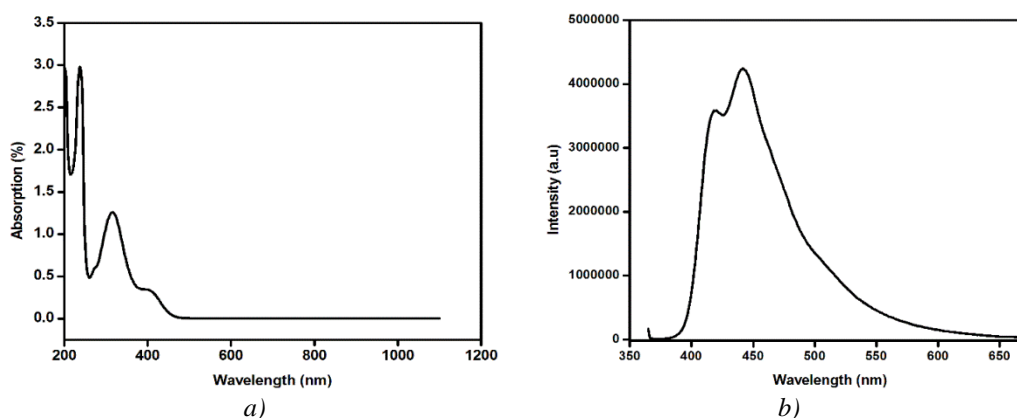


Fig. 8. a) Excitation spectrum of 4n8Q crystal.
b) Emission spectrum of 4n8Q crystal.

DC conductivity

DC electrical conductivity for the grown crystals were carried out using the Keithley 6517B electrometer at various temperatures (303 K to 363 K). The observations were made while cooling the sample. Fig. 9a shows the current–voltage response for the crystals. From the graph it is identified that the current was linearly increasing with the applied voltage. Moreover the current increased with respect to the temperature. DC conductivity was calculated using the given formula

$$\sigma_{dc} = \frac{d}{RA} \quad (4)$$

where, d is the thickness of the sample, R is the measured resistance and A is the area of the face in contact with the electrode. Fig. 9b shows that electrical conductivity linearly increased with the increase in temperature and it confirms the semi conductor nature of the crystal. When the temperature increases, defects will be created inside the crystal. The defect concentration furthermore increases with increase in temperature, thus increasing the conductivity. The increase of conductivity with increasing temperature is attributed to “thermal activated behavior” [42-44]. Fig. 9c depicts the $(\ln(\sigma_{dc}) \text{ Vs } 1000/T)$ ohmic behavior. The conductivity values were fitted with the equation below and the activation energy was calculated. The calculated activation energy is 0.047 eV.

$$\sigma = \sigma_o \exp\left(\frac{-E}{kT}\right) \quad (5)$$

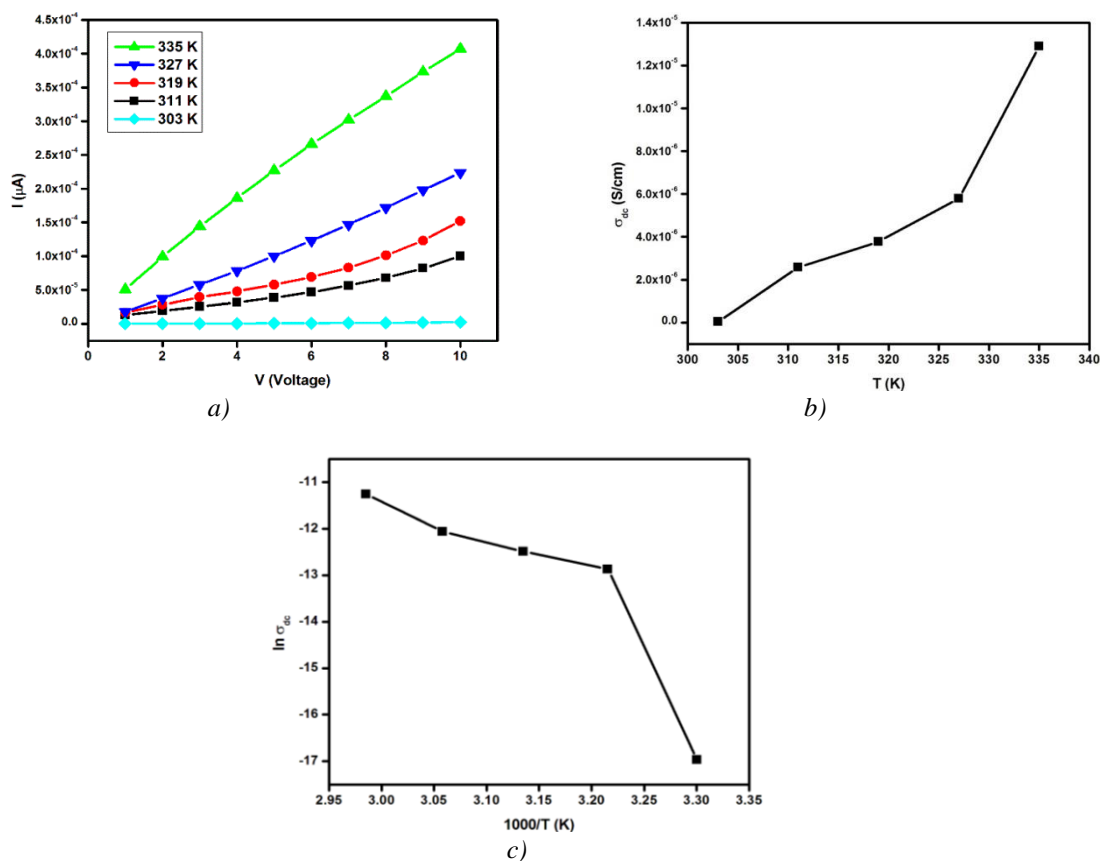


Fig. 9. a) I-V response of of 4n8Q crystal.
 b) Conductivity Vs temeparture for 4n8Q crystal.
 c) $\ln \sigma_{dc}$ Vs $1000/T$ for 4n8Q crystal.

Powder SHG measurement

The optical second harmonic generation behavior of the 4n8Q crystal was tested by the modified Kurtz and Perry technique [45]. The grown crystals were ground well into powder using mortar and pestle. The powder sample was densely packed in a micro capillary tube and exposed to laser radiation. High intense Q-Switched Nd:YAG laser (Quanta – Ray, spectra Physics) with output wavelength of 1064 nm is used. Frequency repetition of 10Hz and a pulse rate of 8ns were passed through the powdered sample. The SHG behavior of the compound was confirmed from the green light emission (532 nm). The input beam energy was measured using power meter and it is 3mJ/pulse. The relative SHG signal outputs are 11mV and 86mV for KDP and 4n8Q respectively. The optical green output was detected by a photomultiplier tube and converted into voltage output at oscilloscope. The SHG efficiency of the 4n8Q compound was compared to standard KDP and it is found to be 7.81 times greater than that of standard KDP.

4. Conclusions

Good quality crystals of 4n8Q were grown by slow evaporation solution growth technique at room temperature. Compositional percentage of the elements were confirmed though CHN analysis. Single crystal XRD confirms that grown crystal belongs to the triclinic system. Powder XRD shows the crystalline nature of the sample. Functional groups present in the system were identified using FTIR technique. Optical transmission study shows above 90 % transparency. Low value of dielectric loss confirms the sample quality. Photoconductivity study reveals the positive nature of the crystal. In powder SHG studies title compound is 7.81 times greater than KDP.

Fluorescence studies reveal the blue fluorescence emission. All above results indicate that 4n8Q can be used as potential of optoelectronic applications.

References

- [1] S. Aruna, M. Vimalan, P. C. Thomas, Tamizharasan, K. Ambujam, J. Madhavan, P. Sagayaraj, *Cryst. Res. Technol.* **42**, 180 (2007).
- [2] J. Chandrasekaran, B. Babu, S. Balaprabhakaran, P. Ilayabarathi, P. Maadeswaran, Sathishkumar K., *Optik* **124**, 1250 (2013).
- [3] L. Guru Prasad, V. Krishnakumar, R. Nagalakshmi, *Physica B.* **405**, 1652 (2010).
- [4] J. Chandrasekaran, B. Babu, S. Balaprabhakaran, *Growth, Optik* **124**, 4296 (2013).
- [5] S. Dhanuskodi, S. Manivannan, K. Kirschbacum, Philip J, Selladurai S. *Structural, J Cryst growth.* **290**, 548 (2006).
- [6] L. Guru Prasad, V. Krishnakumar, R. Nagalakshmi, *Spectrochim Acta Part A.***110**, 377 (2013).
- [7] R. Uthrakumar, C. Vesta, R. Robert, G. Mangalam, S. Jerome Das, *Physica B.* **405**, 4274 (2010).
- [8] B. Milton Boaz, S. Jerome Das, *J. Cryst. Growth* **279**, 383 (2005).
- [9] Tianliang Chen, Zhihua Sun, Cheng Song, Yan Ge, Junhua Luo, Wenxiong Lin, Maochun Hong, *Cryst Growth Des.* **12**, 2673 (2012).
- [10] P. Srinivasan, T. Kanagasekaran, N. Vijayan, G. Bhagavannarayana, R. Gopalakrishnan, P. Ramasamy, *Opt Mater.* **30**, 553 (2007).
- [11] V. Krishnakumar, M. Rajaboopathi, R. Nagalakshmi, *Physica B.* **407**, 1119 (2012).
- [12] G. Anandha babu, R. Perumal Ramasamy, P. Ramasamy, *Mater. Chem. Phys.* **117**, 326 (2009).
- [13] M. Jose, B. Sridhar, G. Bhagavannarayana, K. Sugandhi, R. Uthrakumar, C. Justin Raj, D. Tamilvendhan, S. Jerome Das, *J. Cryst. Growth.* **312**, 793 (2010).
- [14] B. Dhanalakshmi, S. Ponnusamy, C. Muthamizhchelvan, *J. Cryst. Growth.* **313**, 30 (2010).
- [15] L. N. Wang, X. Q. Wang, G. H. Zhang, X. T. Liu, Z. H. Sun, G. H. Sun, Wang L, W. T. Yu, D. Xu, *J. Cryst. Growth.* **327**, 133 (2011).
- [16] Prakash M, Lydia Caroline M, Geetha D., *Spectrochim Acta Part A.* **108**, 32 (2013).
- [17] Krishna Kumar V, Nagalakshmi R, *Spectrochim Acta Part A.* **66**, 924 (2007).
- [18] Basoglu A, Avci D, Atalay A, Celik F, Sahinbas T, *Spectrochim Acta Part A.* **79**, 1425 (2011).
- [19] Peramaiyan G, Pandi P, Vijayan N, Bhagavannarayana G, Mohan Kumar R, *J. Cryst. Growth.* **375**, 6 (2013).
- [20] Krishnakumar V, Nagalakshmi R, Janaki P, *Spectrochim Acta Part A.* **61**, 1097 (2005).
- [21] Prabhakaran SP, Ramesh Babu R, Velusamy P, Ramamurthi K, *Mater Res Bull.* **46**, 1781 (2011).
- [22] Rajasekaran M, Anbusrinivasan P, Mojumdar S C, *J. Therm. Anal. Calorim.* **100**, 827 (2010).
- [23] Kulkarni GU, Kumaradhas P and Rao CNR, *Chem. Mater.* **10**, 3498 (1998).
- [24] Roychowdhur P, *Acta Cryst B.* **34**, 1047 (1978).
- [25] Senthil Pandian M, Pattanaboonmee N, Ramasamy P, Manyum P, *J. Cryst. Growth.* **314**, 207 (2011).
- [26] Senthil Pandian M, Boopathi K, Ramasamy P, Bhagavannarayana G, *Mater Res Bull.* **47**, 826 (2012).
- [27] Senthil Pandian M, Ramasamy P, Binay Kumar P, *Mater Res Bull.* **47**, 1587 (2012).
- [28] Senthil Pandian M, Ramasamy P, *Mater Chem Phys.* **132**, 1019 (2012).
- [29] Shanmugam G, Ravi Kumar K, Sridhar B, Brahadeeswaran S., *Mater Res Bull.* **47**, 2315 (2012).
- [30] Mary Linet J, Jerome Das S., *Mater Chem Phys.* **126**, 886 (2011).
- [31] G. Ganesh G, Ramadoss A, Kannan PS, SubbiahPandi A., *J Therm. Anal. Calorim.* **112**, 547 (2013).
- [32] Neeti Goel, Nidhi Sinha, Binay Kumar, *Opt Mater.* **35**, 479 (2013).

- [33] Babu B, Chandrasekaran J, Balaprabhakaran S, Ilayabarathi P., *Mater-Sci Poland*. **31**, 151 (2013).
- [34] Krishnan P, Gayathri K, Bhagavannarayana G, Gunasekaran S, Anbalagan G., *Spectrochimica Acta part A*. **102**, 379 (2013).
- [35] Prakash M, Geetha D, Lydia Caroline M., *Spectrochimica Acta part A*. **107**, 16 (2013).
- [36] Arjunan S, Bhaskaran A, Mohan Kumar R, Mohan R and Jayavel R, *Mater. Manuf. Process*. **27**, 49 (2012).
- [37] Shanmugam G, Thirupugalmani K, Rakhikrishna R, Philip J, Brahadeeswaran S, *J. Therm. Anal. Calorim.* **114**, 1245 (2013).
- [38] Von Hundelshausen U, *Phys Lett A*. **34**, 405 (1971).
- [39] Milton Boaz B, Mary Navis Priya S, Mary Linet J, Martin Deva Prasath P, Jerome Das S. *Opt Mater.* **29**, 827 (2007).
- [40] N. Vijayan, G. Bhagavannarayana, K. K. Maurya, S. Pal, S. N. Datta, R. Gopalakrishnan and P. Ramasamy, *Cryst. Res. Technol.* **42**, 195 (2007).
- [41] Jose M, Uthrakumar R, Jeya Rajendran A, Jerome Das S., *Spectrochimica Acta part A*. **86**, 495 (2012).
- [42] Parvatikar N, Jain S, Bhoraskar SV, *J Appl Polym Sci*. **102**, 5533 (2006).
- [43] Freeda TH, Mahadevan C., *Bull Mater Sci*. **23**, 335 (2000).
- [44] Ananda Kuamari R, Chandramani R., *Indian J Pure Appl Phys.* **43**, 123 (2005).
- [45] Kurtz SK, Perry TT., *J Appl Phys*. **39**, 3798 (1968).